

# Chapter 9

## Embedded GOE Ensembles for Interacting Boson Systems: BEGOE(1 + 2) for Spinless Bosons

In Chaps. 4–8 EE for fermion systems are discussed in detail with analytical and numerical results. In the present chapter and the next chapter, we will consider EE for finite interacting boson systems (called BEE with ‘B’ for bosons). Unlike for fermion systems, for fixed number ( $N$ ) of sp states, boson number  $m$  can increase beyond  $N$  and therefore a dense limit with  $m \rightarrow \infty$  (complete definition given ahead) is possible and this is one new aspect of boson systems. Also, BEE are important because of the increasing interest in investigating (using experiments and theory) BEC and quantum gases in general. As Asaga et al. state [1]: *In an atomic trap, bosonic atoms occupy partly degenerate single particle states. The interaction will lift the degeneracy. A random matrix approach should reveal the generic features of the resulting system.* In addition, BEE are also important in understanding certain aspects of the Interacting Boson Model (IBM) of atomic nuclei [2–5]. To get started with BEE, we will first consider BEGOE(1 + 2) for spinless boson systems in this chapter.

### 9.1 Definition and Construction

The BEGOE(2)/BEGUE(2) ensemble for spinless boson systems is generated by defining the two-body Hamiltonian  $H$  to be GOE/GUE in two-particle spaces and then propagating it to many-particle spaces by using the geometry of the many-particle spaces [this is in general valid for  $k$ -body Hamiltonians, with  $k < m$ , generating BEGOE( $k$ )/BEGUE( $k$ )]. Consider a system of  $m$  spinless bosons occupying  $N$  sp states  $|v_i\rangle$ ,  $i = 1, 2, \dots, N$ ; see Fig. 9.1. Then, BEGOE(2) is defined by the Hamiltonian operator,

$$\hat{H}(2) = \sum_{v_i \leq v_j, v_k \leq v_l} \frac{\langle v_k v_l | \hat{H}(2) | v_i v_j \rangle}{\sqrt{(1 + \delta_{ij})(1 + \delta_{kl})}} b_{v_k}^\dagger b_{v_l}^\dagger b_{v_i} b_{v_j}, \quad (9.1)$$

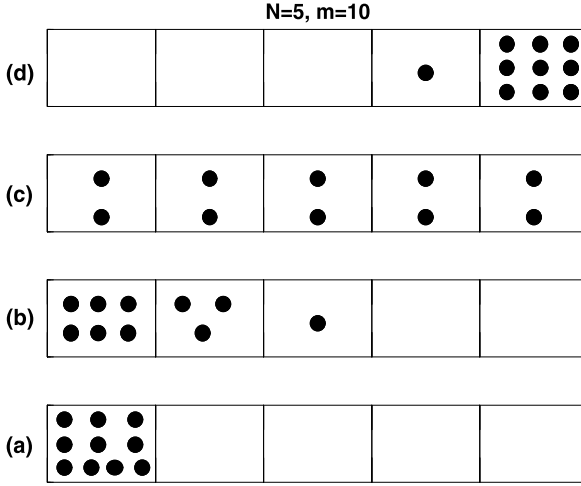


**Fig. 9.1** Some  $m$  boson configurations or basis states for  $m = 10$  spinless bosons in  $N = 5$  sp states. Enumeration of the configurations is similar to distributing  $m$  particles in  $N$  boxes with the conditions that the occupancy of each box lies between zero and  $m$  and the maximum number of occupied boxes equals  $m$ . In the figure, (a) corresponds to the basis state  $|(v_1)^{10}\rangle$ , (b) corresponds to the basis state  $|(v_1)^6(v_2)^3v_3\rangle$ , (c) corresponds to the basis state  $|(v_1)^2(v_2)^2(v_3)^2(v_4)^2(v_5)^2\rangle$  and (d) corresponds to the basis state  $|v_4(v_5)^9\rangle$

with the symmetries for the symmetrized two-body matrix elements  $\langle v_k v_l | \widehat{H}(2) | v_i v_j \rangle$  being,

$$\begin{aligned} \langle v_k v_l | \widehat{H}(2) | v_j v_i \rangle &= \langle v_k v_l | \widehat{H}(2) | v_i v_j \rangle, \\ \langle v_k v_l | \widehat{H}(2) | v_i v_j \rangle &= \langle v_i v_j | \widehat{H}(2) | v_k v_l \rangle. \end{aligned} \quad (9.2)$$

Note that  $|v_i v_j\rangle$  denote two-boson symmetric states. The action of the Hamiltonian operator defined by Eq. (9.1) on the basis states, defined by distributions of bosons in the sp states as shown in Fig. 9.1, generates the  $H$  matrix in  $m$ -boson spaces. Note that  $b_{v_i}$  and  $b_{v_i}^\dagger$  in Eq. (9.1) annihilate and create a boson in the sp state  $|v_i\rangle$ , respectively. The Hamiltonian matrix  $H(m)$  in  $m$ -particle spaces contains three different types of non-zero matrix elements and explicit formulas for these are [6],

$$\begin{aligned} \left\langle \prod_{r=i,j,\dots} (v_r)^{n_r} \widehat{H}(2) \left| \prod_{r=i,j,\dots} (v_r)^{n_r} \right\rangle &= \sum_{i \geq j} \frac{n_i(n_j - \delta_{ij})}{(1 + \delta_{ij})} \langle v_i v_j | \widehat{H}(2) | v_i v_j \rangle, \\ \left\langle (v_i)^{n_i-1} (v_j)^{n_j+1} \prod_{r'=k,l,\dots} (v_{r'})^{n_{r'}} \widehat{H}(2) \left| \prod_{r=i,j,\dots} (v_r)^{n_r} \right\rangle \right. \\ &= \sum_{k'} \left[ \frac{n_i(n_j + 1)(n_{k'} - \delta_{k'i})^2}{(1 + \delta_{k'i})(1 + \delta_{k'j})} \right]^{1/2} \langle v_{k'} v_j | \widehat{H}(2) | v_k v_i \rangle, \end{aligned} \quad (9.3)$$

$$\begin{aligned} & \left\langle (v_i)^{n_i+1} (v_j)^{n_j+1} (v_k)^{n_k-1} (v_l)^{n_l-1} \prod_{r'=m,n,\dots} (v_{r'})^{n_{r'}} \left| \widehat{H}(2) \right| \prod_{r=i,j,\dots} (v_r)^{n_r} \right\rangle \\ &= \left[ \frac{n_k(n_l - \delta_{kl})(n_i + 1)(n_j + 1 + \delta_{ij})}{(1 + \delta_{ij})(1 + \delta_{kl})} \right]^{1/2} \langle v_i v_j | \widehat{H}(2) | v_k v_l \rangle. \end{aligned}$$

Note that all other  $m$ -particle matrix elements are zero due to two-body selection rules. In the second equation in Eq. (9.3),  $i \neq j$  and in the third equation, four combinations are possible: (i)  $k = l, i = j, k \neq i$ ; (ii)  $k = l, i \neq j, k \neq i, k \neq j$ ; (iii)  $k \neq l, i = j, i \neq k, i \neq l$ ; and (iv)  $i \neq j \neq k \neq l$ . BEGOE(2) for spinless boson systems is defined by Eqs. (9.2) and (9.3) with the  $H$  matrix in two-particle spaces represented by  $\text{GOE}(v^2)$ . Now the  $m$ -boson BEGOE(2) Hamiltonian matrix ensemble is denoted by  $\{H(m)\}$ , with  $\{H(2)\}$  being a GOE. Note that the  $H(m)$  matrix dimension is

$$d_b(N, m) = \binom{N + m - 1}{m} \tag{9.4}$$

and the number of independent matrix elements is  $d_b(N, 2)[d_b(N, 2) + 1]/2$ . The subscript ‘ $b$ ’ in  $d_b(N, m)$  stands for ‘bosons’. Using Eqs. (9.2) and (9.3) with GOE representation for  $H$  in two-particle spaces, computer codes have been developed for constructing BEGOE(2) ensemble [7].

Extension of BEGOE(2) to BEGOE(1 + 2) incorporating mean-field one-body part is straightforward. The BEGOE(1 + 2) Hamiltonian is,

$$\{\widehat{H}\}_{\text{BEGOE}(1+2)} = \widehat{h}(1) + \lambda \{\widehat{V}(2)\}; \quad \widehat{h}(1) = \sum_{i=1}^N \varepsilon_i \widehat{n}_i. \tag{9.5}$$

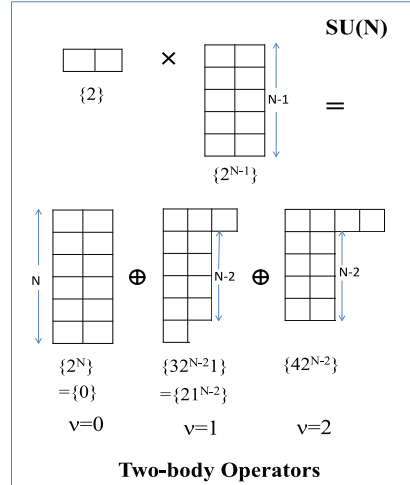
The  $\widehat{V}(2)$  above is same as  $\widehat{H}(2)$  in Eq. (9.1) and the two-particle matrix elements of  $\widehat{V}(2)$  are  $V_{ijkl} = \langle i, j | \widehat{V}(2) | k, l \rangle$ . Similarly,  $\varepsilon_i$  in Eq. (9.5) are sp energies and they can be fixed or drawn from an appropriate random ensemble as in EGOE(1 + 2). Now on, we will drop the hat over  $H, h$  and  $V$  when there is no confusion. The  $m$  particle matrix for  $H$  in Eq. (9.5) follows from Eqs. (9.2) and (9.3) by just adding the  $h(1)$  contribution to the diagonal matrix elements,

$$\left\langle \prod_{r=i,j,\dots} (v_r)^{n_r} \left| h(1) \right| \prod_{r=i,j,\dots} (v_r)^{n_r} \right\rangle = \sum_{r=i,j,\dots} n_r \varepsilon_r. \tag{9.6}$$

We assume that the sp energies given by  $h(1)$  have average spacing  $\Delta$ . The  $\lambda$  parameter is expressed in units of  $\Delta$  and we assume without loss of generality  $\Delta = 1$ . Clearly, it is easy to construct BEGOE(1 + 2) matrices on a computer using the code for BEGOE(2). However, the matrix dimensions makes the calculations prohibitive for larger vales of  $(m, N)$ . For example  $d_b(5, 10) = 1001, d_b(6, 12) = 6188, d_b(6, 20) = 53130, d_b(8, 20) = 888030$  and  $d_b(10, 20) = 10015005$ .

It is important to stress that, unlike for fermionic EE, there are only a few BEE investigations in literature [1, 6, 8–11]. Moreover, for interacting spinless boson

**Fig. 9.2** Young tableaux for various tensor parts of two-body operators with respect to  $SU(N)$  for spinless boson systems. Figure 5.1a gives the tensor parts for one-body operators (Color figure online)



systems with  $m$  bosons in  $N$  sp orbitals, dense limit defined by  $m \rightarrow \infty$ ,  $N \rightarrow \infty$  and  $m/N \rightarrow \infty$  is also possible as  $m$  can be greater than  $N$  for bosons. Also, many of the results for bosons, as discussed ahead, can be obtained from those for fermions by using  $N \rightarrow -N$  symmetry and a  $m \rightarrow N$  symmetry [12–15].

Using BEGOE(1 + 2) codes, in many numerical examples, eigenvalue densities  $\rho(E)$  are constructed and they are seen to be close to Gaussian in form. Due to growing matrix dimensions, most of the calculations are restricted to  $N = 4, 5$  with  $m = 10\text{--}12$  giving reasonable examples for the dense limit [6, 9, 16]. See Fig. 5.2 for an example. In order to further confirm that  $\rho(E)$  is close to Gaussian for BEGOE(1 + 2), analytical formulas for the first four moments of the eigenvalue density are derived for a given  $\widehat{H}(1 + 2)$ . Before turning to them it is useful to mention that a more symmetrized form of  $V_{ijkl}$  will be useful and to this end introduced are  $\mathcal{V}_{ijkl}$  where

$$\mathcal{V}_{ijkl} = \sqrt{(1 + \delta_{ij})(1 + \delta_{kl})} V_{ijkl}. \tag{9.7}$$

Then, the  $V(2)$  operator takes the form

$$V(2) = \frac{1}{4} \sum_{i,j,k,l} \mathcal{V}_{ijkl} b_i^\dagger b_j^\dagger b_k b_l. \tag{9.8}$$

In the next two subsections  $\lambda V(2)$  is called  $V(2)$ .

## 9.2 Energy Centroids and Spectral Variances: $U(N)$ Algebra

Embedding algebra for BEGOE(1 + 2) is  $U(N)$ . As one and two boson states transform the  $U(N)$  irreps  $\{1\}$  and  $\{2\}$  in Young tableaux notation, the one and two boson

creation operators also transform as  $\{1\}$  and  $\{2\}$ . Then, one and two boson annihilation operators transform as  $\{1^{N-1}\}$  and  $\{2^{N-1}\}$  respectively. Therefore,  $h(1)$  transform as  $\{1\} \times \{1^{N-1}\} = [\{1^N\} = \{0\}] \oplus \{21^{N-2}\} = (\nu = 0) + (\nu = 1)$  irreps (or tensors). Note that here we have used  $U(N) \leftrightarrow SU(N)$  equivalence. Similarly  $V(2)$  transforms as  $\{2\} \times \{2^{N-1}\} = [\{2^N\} = \{0\}] \oplus [\{32^{N-2}1\} = \{21^{N-2}\}] \oplus \{42^{N-2}\} = (\nu = 0) + (\nu = 1) + (\nu = 2)$  irreps (or tensors). Figures 5.1a and 9.2 show these decompositions in terms of Young tableaux for one-body and two-body operators respectively. Given  $H = h(1) + V(2)$  as defined by Eqs. (9.5)–(9.8), it is possible to write explicitly its  $U(N)$  decomposition into various  $\nu$  parts. Firstly, it is easy to recognize the  $\nu = 0$  part as it should be a scalar with respect to  $U(N)$ , i.e. it should be a polynomial in  $\hat{n}$ . The result is,

$$H^{\nu=0}(1+2) = h^{\nu=0}(1) + V^{\nu=0}(2) = \varepsilon_0 \hat{n} + V_0 \binom{\hat{n}}{2};$$

$$\varepsilon_0 = \frac{1}{N} \sum_i \varepsilon_i, \quad V_0 = \frac{1}{2N(N+1)} \sum_{i,j} \mathcal{Y}_{ijij}. \quad (9.9)$$

Little thought will give the  $\nu = 1$  parts of  $h(1)$  and  $V(2)$ ,

$$H^{\nu=1}(1+2) = h^{\nu=1}(1) + V^{\nu=1}(2),$$

$$h^{\nu=1}(1) = \sum_i \varepsilon_i^{\nu=1} \hat{n}_i; \quad \varepsilon_i^{\nu=1} = \varepsilon_i - \varepsilon_0,$$

$$V^{\nu=1}(2) = (\hat{n} - 1) \sum_{i,j} \zeta_{i,j} b_i^\dagger b_j; \quad (9.10)$$

$$\zeta_{i,j} = \frac{1}{N+2} \sum_k \left( \mathcal{Y}_{ikjk} - \delta_{ij} \frac{1}{N} \left[ \sum_{m,n} \mathcal{Y}_{mnmn} \right] \right).$$

Thus,  $V^{\nu=1}$  corresponds to an effective ( $m$ -dependent) mean-field producing part of  $V(2)$  and it is in general off-diagonal in the original mean-field basis, i.e.  $\zeta_{ij} \neq 0$  for  $i \neq j$ . Finally,  $V^{\nu=2}(2)$  part is given by

$$V^{\nu=2}(2) = V(2) - V^{\nu=0}(2) - V^{\nu=1}(2);$$

$$V_{ijij}^{\nu=2} = V_{ijij} - V_0 - \zeta_{i,i} - \zeta_{j,j}, \quad (9.11)$$

$$V_{ikjk}^{\nu=2} = V_{ikjk} - \sqrt{(1 + \delta_{ik})(1 + \delta_{jk})} \zeta(i, j); \quad i \neq j,$$

$$V_{ijkl}^{\nu=2} = V_{ijkl}; \quad \text{for all other cases.}$$

Also, we can write the  $V^{\nu=2}(2)$  operator as

$$V^{\nu=2}(2) = \frac{1}{4} \sum_{i,j,k,l} \tilde{\mathcal{Y}}_{ijkl} b_i^\dagger b_j^\dagger b_k b_l; \quad \tilde{\mathcal{Y}}_{ijkl} = \sqrt{(1 + \delta_{ij})(1 + \delta_{kl})} V_{ijkl}^{\nu=2}. \quad (9.12)$$

Just as for fermion systems, propagation equation for boson systems for the  $m$ -particle average of a  $k$ -body operator  $A(k)$  is simple,

$$\langle A(k) \rangle^m = \binom{m}{k} \langle A(k) \rangle^k. \quad (9.13)$$

Similarly, the various  $v$  parts of  $A(k)$  will be orthogonal with respect to averages over the  $m$ -boson spaces, i.e.  $\langle A^{v_1} B^{v_2} \rangle^m = \delta_{v_1 v_2} \langle A^{v_1} B^{v_1} \rangle^m$ . As the  $m$  particle averages are polynomials in  $m$ , using Eq. (9.13) we obtain easily the propagation equations for the energy centroids and spectral variances,

$$\begin{aligned} E_c(m) &= \langle H(1+2) \rangle^m = m\varepsilon_0 + \binom{m}{2} V_0, \\ \sigma^2(m) &= \langle (H - H^{v=0})^2 \rangle^m = \langle (H^{v=1})^2 \rangle^m + \langle (H^{v=2})^2 \rangle^m; \\ \langle (H^{v=1})^2 \rangle^m &= \frac{m(m+N)}{N(N+1)} \sum_{i,j} \xi_{ij}(m) \xi_{ji}(m), \\ \xi_{ij}(m) &= \varepsilon_i^{v=1} \delta_{ij} + (m-1) \xi_{ij}, \end{aligned} \quad (9.14)$$

$$\langle (H^{v=2})^2 \rangle^m = \frac{m(m-1)(N+m)(N+m+1)}{N(N+1)(N+2)(N+3)} \frac{1}{4} \sum_{i,j,k,l} \tilde{\mathcal{V}}_{ijkl} \tilde{\mathcal{V}}_{klij}.$$

Using Eq. (9.14) we can calculate ensemble average values for the energy centroids (they come from  $h(1)$  only) and spectral variances for any  $m$  and with these, Gaussian eigenvalue densities can be constructed. However, to prove that the dense limit gives Gaussian form, formulas for the third and fourth moments are needed as discussed below.

### 9.3 Third and Fourth Moment Formulas: Gaussian Eigenvalue Density in Dense Limit

For fermion systems, formulas for the third and fourth moments  $\langle (H - H^{v=0})^i \rangle^m$ ,  $i = 3, 4$  are derived in detail by several authors using diagrammatic methods [17, 18]. They can be extended to boson systems by using  $N \rightarrow -N$  symmetry [12–15], i.e. by substituting  $-N$  for  $N$  in the expressions for moments of fermion systems and then taking absolute values of each term, one obtains the expressions for boson systems. The final formulas for 3rd and 4th moments are [12] as follows. Firstly,

formula for the 3rd central moment is

$$\begin{aligned}
\mathcal{M}_3 &= \langle (H - H^{v=0})^3 \rangle^m \\
&= \frac{m(N+m)(N+2m)}{N(N+1)(N+2)} X_1 \\
&\quad + \sum_{s=2,3} \binom{m}{s} \binom{N+m+1}{2} \binom{s+2}{2}^{-1} \binom{N+s+1}{s+2}^{-1} X_s + \langle (\tilde{\mathcal{V}})^3 \rangle^m; \\
X_1 &= \sum_{i,j,k} \xi_{ij}(m) \xi_{jk}(m) \xi_{ki}(m), \quad X_2 = 3D_1 + \frac{3}{2}E_1, \quad X_3 = 3E_1, \\
D_1 &= \sum_{i,j,k,l} \tilde{\mathcal{V}}_{ijkl} \xi_{ik}(m) \xi_{jl}(m), \\
E_1 &= \sum_{i,j,k,l,r} \tilde{\mathcal{V}}_{ijkl} \tilde{\mathcal{V}}_{krij} \xi_{lr}(m).
\end{aligned} \tag{9.15}$$

Formula for  $\langle (\tilde{\mathcal{V}})^3 \rangle^m$  is given ahead. Going further, formula for the fourth central moment is,

$$\begin{aligned}
\mathcal{M}_4 &= \langle (H - H^{v=0})^4 \rangle^m \\
&= \frac{m(N+m)}{N(N+1)} M_2 + \sum_{s=2,3} \binom{m}{s} \binom{N+m+1}{2} \binom{s+2}{2}^{-1} \binom{N+s+1}{s+2}^{-1} Y_s \\
&\quad + \sum_{s=2,3} \binom{m}{s+1} \binom{N+m+2}{3} \binom{s+4}{3}^{-1} \binom{N+s+3}{s+4}^{-1} Z_s + \langle (\tilde{\mathcal{V}})^4 \rangle^m; \\
Y_2 &= 12K_1 + 2(G_1 + G_2 + G_3) + F_1 + 3(M_1)^2 + 6M_2, \\
Y_3 &= 24K_1 + 2F_1, \\
Z_2 &= 12G_1 + 6G_2 + 12G_3 + 12G_4 + \frac{3}{2}G_5 + 2F_1 + 12F_2 + 6F_3, \\
Z_3 &= 4F_1 + 24F_2 + 12F_3, \\
M_1 &= \sum_{i,j} \xi_{ij}(m) \xi_{ji}(m), \quad M_2 = \sum_{i,j,k,l} \xi_{ij}(m) \xi_{jk}(m) \xi_{kl}(m) \xi_{li}(m), \\
K_1 &= \sum_{i,j,k,l,r} \tilde{\mathcal{V}}_{ijkl} \xi_{ik}(m) \xi_{jr}(m) \xi_{rl}(m), \\
G_1 &= \sum_{i,j,k,l,r,s} \tilde{\mathcal{V}}_{ijkl} \tilde{\mathcal{V}}_{ksij} \xi_{ir}(m) \xi_{rs}(m), \quad G_2 = \sum_{i,j,k,l,r,s} \tilde{\mathcal{V}}_{ijkl} \tilde{\mathcal{V}}_{rsij} \xi_{kr}(m) \xi_{ls}(m), \\
G_3 &= \sum_{i,j,k,l,r,s} \tilde{\mathcal{V}}_{ijkl} \tilde{\mathcal{V}}_{kris} \xi_{lr}(m) \xi_{sj}(m), \quad G_4 = \sum_{i,j,k,l,r,s} \tilde{\mathcal{V}}_{ijkl} \tilde{\mathcal{V}}_{kris} \xi_{jl}(m) \xi_{rs}(m),
\end{aligned}$$

$$\begin{aligned}
G_5 &= \left[ \sum_{i,j,k,l} \tilde{\mathcal{V}}_{ijkl} \tilde{\mathcal{V}}_{klij} \right] \left[ \sum_{r,s} \xi_{rs}(m) \xi_{sr}(m) \right], \\
F_1 &= \sum_{i,j,k,l,r,s,p} \tilde{\mathcal{V}}_{ijkl} \tilde{\mathcal{V}}_{kprs} \tilde{\mathcal{V}}_{rsij} \xi_{lp}(m), & F_2 &= \sum_{i,j,k,l,r,s,p} \tilde{\mathcal{V}}_{ijkl} \tilde{\mathcal{V}}_{lrjs} \tilde{\mathcal{V}}_{spri} \xi_{kp}(m), \\
F_3 &= \sum_{i,j,k,l,r,s,p} \tilde{\mathcal{V}}_{ijkl} \tilde{\mathcal{V}}_{klrj} \tilde{\mathcal{V}}_{rpi} \xi_{sp}(m).
\end{aligned} \tag{9.16}$$

Finally, formula for  $\langle \tilde{\mathcal{V}}^r \rangle^m$ , valid for  $r = 2, 3$  and  $4$ , is given by

$$\begin{aligned}
\langle (\tilde{\mathcal{V}}^r)^m \rangle &= \sum_{s=2}^r \binom{m}{s} \binom{N+s+m-1}{s} \binom{2s}{s}^{-1} \binom{N+2s-1}{2s}^{-1} C_r^s; \\
C_2^2 &= \frac{1}{4} \sum_{i,j,k,l} \tilde{\mathcal{V}}_{ijkl} \tilde{\mathcal{V}}_{klij}, & C_3^2 &= \frac{1}{8} \sum_{i,j,k,l,r,s} \tilde{\mathcal{V}}_{ijkl} \tilde{\mathcal{V}}_{klrs} \tilde{\mathcal{V}}_{rsij}, \\
C_3^3 &= 2C_3^2 + \sum_{i,j,k,l,r,s} \tilde{\mathcal{V}}_{iljk} \tilde{\mathcal{V}}_{kslr} \tilde{\mathcal{V}}_{rj} \tilde{\mathcal{V}}_{rsi}, & C_4^2 &= \frac{1}{16} (AA1), \\
C_4^3 &= \frac{1}{4} (AA1) + (CC1) + \frac{1}{2} (BA1) + 2(CA1), \\
C_4^4 &= \frac{3}{8} (AA1) + 6(CC1) + 3(BA1) + 6(CA1) + 3(AB1) + 3(C_2^2)^2, \tag{9.17} \\
AA1 &= \sum_{i,j,k,l,r,s,o,p} \tilde{\mathcal{V}}_{ijkl} \tilde{\mathcal{V}}_{klrs} \tilde{\mathcal{V}}_{rsop} \tilde{\mathcal{V}}_{opij}, \\
AB1 &= \sum_{i,j,k,l,r,s,o,p} \tilde{\mathcal{V}}_{ijkl} \tilde{\mathcal{V}}_{lrjs} \tilde{\mathcal{V}}_{sorp} \tilde{\mathcal{V}}_{pkoi}, \\
BA1 &= \sum_{i,j,k,l,r,s,o,p} \tilde{\mathcal{V}}_{ijkl} \tilde{\mathcal{V}}_{klis} \tilde{\mathcal{V}}_{rsop} \tilde{\mathcal{V}}_{oprj}, \\
CA1 &= \sum_{i,j,k,l,r,s,o,p} \tilde{\mathcal{V}}_{ijkl} \tilde{\mathcal{V}}_{krso} \tilde{\mathcal{V}}_{olrp} \tilde{\mathcal{V}}_{spij}, \\
CC1 &= \sum_{i,j,k,l,r,s,o,p} \tilde{\mathcal{V}}_{ijkl} \tilde{\mathcal{V}}_{rsjo} \tilde{\mathcal{V}}_{olsp} \tilde{\mathcal{V}}_{pkri}.
\end{aligned}$$

By numerical construction of various members of BEGOE(1 + 2) with some values for  $(m, N, \lambda)$ , formulas given by Eqs. (9.14)–(9.17) have been verified and they in turn provide a good test of the BEGOE(1 + 2) codes. Some examples are as follows [19]. For  $m = 8, 12, 20$  and  $400$  with  $N = 5$ ,  $\overline{\gamma}_2$  values are  $-0.21, -0.11, -0.05$  and  $-0.03$  respectively. Similarly, for  $m = 12, 20$  and  $400$  with  $N = 12$ , the  $\overline{\gamma}_2$  values are  $-0.17, -0.07$  and  $-0.01$  respectively. For sufficiently large values for  $N$  ( $N > 5$ ) and  $m \gg N$ ,  $|\overline{\gamma}_2| < 0.3$  ( $\overline{\gamma}_1 \sim 0$  as expected) for BEGOE(2). Analytical formula for  $\overline{\gamma}_2$  can be obtained by considering  $V^{\nu=2}(2)$ . In the strict dense limit,



only this part will generate  $\gamma_2$  for BEGOE(2). Equations (9.17) and (9.14) will give,

$$\begin{aligned} \overline{\gamma_2(m, N)} &\xrightarrow{m \rightarrow \infty} \frac{(N+2)(N+3)P}{(N+5)(N+6)(N+7)} - 3; \\ P &= 6 \frac{(N+4)(N+5)^2}{(N+2)(N+3)} [\gamma_2(4, N) + 3] \\ &\quad - 6 \frac{(N+4)(N+6)}{(N+2)} [\gamma_2(3, N) + 3] + (N+7) [\gamma_2(2, N) + 3]. \end{aligned} \quad (9.18)$$

For sufficiently large  $N$ ,  $\gamma_2(m, N)$  for  $m = 2, 3$  and  $4$  will be given by Eq. (4.32), i.e.  $\gamma_2(m) \sim \binom{m}{2}^{-1} \binom{m-2}{2} - 1$ . Then,  $\gamma_2(2, N) = \gamma_2(3, N) = -1$  and  $\gamma_2(4, N) = -5/6$ . These and Eq. (9.18) will lead to

$$\gamma_2(\infty, N) = -2(2N+11)/(N+6)(N+7). \quad (9.19)$$

Therefore in the dense limit [6],

$$\gamma_2 \xrightarrow{\text{dense limit}} -\frac{4}{N} \quad (9.20)$$

and this is good for  $N \geq 20$ . The dense limit result for BEGOE(2) as given by Eq. (9.20) should be compared to the result  $\gamma_2(m) \rightarrow -4/m$  for EGOE(2) for fermions in the dilute limit. Thus there is a  $m \rightarrow N$  symmetry between fermions in dilute limit and bosons in the dense limit. Thus, for sufficiently large values of  $N$ , BEGOE(2) gives Gaussian eigenvalue densities in the dense limit. However, even for small  $N$  as seen from Eq. (9.19), the Gaussian form is valid. For example for  $N = 5$ , we have  $\gamma_2(\infty, N) = -0.32$  and therefore for the dense boson systems  $N > 5$  is sufficient for obtaining the Gaussian form.

Simplifications used above are some what complicated for BEGOE(1 + 2). However, it can be shown easily [12] that reasonable  $h(1)$  will give Gaussian densities in the dense limit. Combining this with the EGOE(2) Gaussian densities, one can argue that BEGOE(1 + 2) in general, independent of  $\lambda$  value, gives Gaussian eigenvalue densities; see Fig. 5.2. Numerical calculations for sufficiently large value for  $N$  ( $N > 5$ ) and  $m \gg N$  have indeed shown that  $|\overline{\gamma_2}| < 0.3$  (similarly  $\overline{\gamma_1}$ ) for BEGOE(1 + 2). Some examples with  $\lambda = 0.025$  and sp energies given by  $\varepsilon_i = i + 1/i$  are as follows [19]. With  $m = 10$ , for  $N = 4, 6$  and  $8$ ,  $(\overline{\gamma_1}, \overline{\gamma_2}) = (0.16, -0.43), (0.13, -0.29)$  and  $(0.09, -0.25)$  respectively. Similarly, With  $m = 5000$ , for  $N = 4, 8$  and  $12$ ,  $(\overline{\gamma_1}, \overline{\gamma_2}) = (0.0, -0.41), (0.0, -0.2)$  and  $(0.0, -0.13)$  respectively.

## 9.4 Average-Fluctuation Separation and Ergodicity in the Spectra of Dense Boson Systems

### 9.4.1 Average-Fluctuation Separation

For boson systems we will consider BEGOE(2) and the dense limit defined by  $m \rightarrow \infty$ ,  $N \rightarrow \infty$  and  $m/N \rightarrow \infty$ . As discussed in Sect. 4.3.1, level motion in BEGOE(2) is given by Eqs. (4.44) and (4.50) as the eigenvalue density in the dense limit is close to a Gaussian. To apply Eq. (4.50), we need  $\tilde{\Sigma}_{rr}$ . A formula for this is obtained as follows.

In two particle space, the  $H$  matrix is GOE and therefore the two particle matrix elements  $H_{\alpha\beta}$  are independent Gaussian variables with  $\overline{H_{\alpha\beta}} = 0$ ,  $\overline{H_{\alpha\alpha}^2} = 2\nu^2$  and  $\overline{H_{\alpha\beta}^2} = \nu^2$  for  $\alpha \neq \beta$ . Now the two particle variance is,

$$\begin{aligned} \overline{\langle H^2 \rangle^{m=2}} &= \binom{N+1}{2}^{-1} \sum_{\alpha, \beta} \overline{H_{\alpha\beta}^2} \\ &= \binom{N+1}{2}^{-1} \left\{ \binom{N+1}{2} \left\{ \binom{N+1}{2} - 1 \right\} \nu^2 + \binom{N+1}{2} 2\nu^2 \right\}. \end{aligned} \quad (9.21)$$

For large  $N$ , the above equation simplifies to  $\overline{\langle H^2 \rangle^{m=2}} = N^2 \nu^2 / 2$ . Therefore the  $m$ -particle variance  $\sigma^2(m)$ , from Eq. (9.14), is

$$\begin{aligned} \sigma^2(m) &= \langle H^2 \rangle^m \rightarrow \langle (H^{\nu=2})^2 \rangle^m \\ &= \frac{m(m-1)(N+m)(N+m+1)}{N(N+1)(N+2)(N+3)} \langle \langle H^2 \rangle \rangle^{m=2}. \end{aligned} \quad (9.22)$$

Then in the dense limit, using the normalization  $\langle H^2 \rangle^{m=2} = \sigma^2(2) = N^2 \nu^2 / 2 = 1$ , we have

$$\sigma^2(m) = \binom{m}{2}^2 \binom{N}{2}^{-1}. \quad (9.23)$$

Now, the variance  $\Sigma_{11}$  of the centroid fluctuations is given by

$$\begin{aligned} \Sigma_{11} &= \overline{\langle H \rangle^m \langle H \rangle^m} - \overline{\langle H \rangle^m} \overline{\langle H \rangle^m} = \overline{\frac{m(m-1)}{N(N+1)} \sum_{\alpha} H_{\alpha\alpha} \frac{m(m-1)}{N(N+1)} \sum_{\beta} H_{\beta\beta}} \\ &= \frac{m^4}{N^4} \sum_{\alpha} \overline{H_{\alpha\alpha}^2} = \frac{m^4}{N^4} \binom{N+1}{2} 2\nu^2 = 2 \frac{m^4}{N^4} \langle H^2(2) \rangle^{m=2} \\ \Rightarrow \tilde{\Sigma}_{11} &= 2 \frac{m^4}{N^4}. \end{aligned} \quad (9.24)$$

In the last step in Eq. (9.24) we have used the normalization that  $\sigma^2(2) = 1$  and also  $\overline{H_{\alpha\alpha}H_{\beta\beta}} = 0$  for  $\alpha \neq \beta$ . Similarly the expression for the variance of the variance fluctuations  $\Sigma_{22} = \langle H^2 \rangle^m \langle H^2 \rangle^m - \overline{\langle H^2 \rangle^m \langle H^2 \rangle^m}$  is derived as follows. First we use

$$\begin{aligned} \langle H^2 \rangle^m &= \frac{m(m-1)(N+m)(N+m+1)}{N(N+1)(N+2)(N+3)} \langle H^2 \rangle^2 \\ &\stackrel{\substack{m \rightarrow \infty, \\ N \rightarrow \infty \\ m/N \rightarrow \infty}}{=} \frac{m^4}{N^4} 2 \sum_{\alpha \geq \beta} H_{\alpha\beta}^2. \end{aligned} \quad (9.25)$$

Then,

$$\begin{aligned} \Sigma_{22} &= 4 \frac{m^8}{N^8} \sum_{\substack{\alpha \geq \beta \\ \gamma \geq \delta}} \overline{H_{\alpha\beta}^2 H_{\gamma\delta}^2} - 4 \frac{m^8}{N^8} \sum_{\alpha \geq \beta} \overline{H_{\alpha\beta}^2} \sum_{\gamma \geq \delta} \overline{H_{\gamma\delta}^2} \\ &= 4 \frac{m^8}{N^8} \left\{ \sum_{\alpha \geq \beta} \overline{H_{\alpha\beta}^4} + \sum_{\substack{\alpha\beta \neq \gamma\delta \\ \alpha \geq \beta \\ \gamma \geq \delta}} \overline{H_{\alpha\beta}^2} \overline{H_{\gamma\delta}^2} - \sum_{\alpha \geq \beta} \overline{H_{\alpha\beta}^2} \sum_{\gamma \geq \delta} \overline{H_{\gamma\delta}^2} \right\} \\ &= 4 \frac{m^8}{N^8} \left\{ \sum_{\alpha \geq \beta} \overline{H_{\alpha\beta}^4} - \sum_{\alpha \geq \beta} \overline{(H_{\alpha\beta}^2)^2} + \sum_{\substack{\alpha \geq \beta \\ \gamma \geq \delta}} \overline{H_{\alpha\beta}^2} \overline{H_{\gamma\delta}^2} - \sum_{\substack{\alpha \geq \beta \\ \gamma \geq \delta}} \overline{H_{\alpha\beta}^2} \overline{H_{\gamma\delta}^2} \right\} \\ &= 4 \frac{m^8}{N^8} \left\{ 3 \sum_{\alpha \geq \beta} v^4 - \sum_{\alpha \geq \beta} v^4 \right\} \\ &= 4 \frac{m^8}{N^8} 2 \left\{ \frac{1}{2} \binom{N+1}{2} \left( \binom{N+1}{2} + 1 \right) \right\} v^4 \\ &\simeq 4 \frac{m^8}{N^8} \left( \langle H^2(2) \rangle^{m=2} \right)^2. \end{aligned} \quad (9.26)$$

Now using the normalization that  $\sigma^2(2) = 1$  gives

$$\tilde{\Sigma}_{22} = 4 \frac{m^8}{N^8}. \quad (9.27)$$

Following Eqs. (9.24) and (9.27), it is conjectured [6] that in general  $\tilde{\Sigma}_{\zeta\zeta}$  is,

$$\tilde{\Sigma}_{\zeta\zeta} = \overline{\langle H^\zeta \rangle^m \langle H^\zeta \rangle^m} = 2\zeta \frac{m^{4\zeta}}{N^{4\zeta}} = 2\zeta \binom{m}{2}^{2\zeta} \binom{N}{2}^{-2\zeta}. \quad (9.28)$$

Note that for a  $k$ -body Hamiltonian, it is plausible that  $\tilde{\Sigma}_{\zeta\zeta} = 2\zeta \binom{m}{k}^{2\zeta} \binom{N}{k}^{-2\zeta}$ . Combining (9.23), (9.28) and (4.50) will give,

$$\overline{(S_\zeta^2)} = 2\zeta \binom{N}{2}^{-\zeta}. \quad (9.29)$$

Substituting this in Eq. (4.44) gives for the level motion in dense limit for BEGOE(2),

$$\begin{aligned} \frac{\overline{(\delta E)^2}}{D(E)^2} \stackrel{\text{BEGOE}(2)}{=} & \binom{N+m-1}{m}^2 \binom{m}{2}^2 \binom{N}{2}^{-2} [\rho_{\mathcal{G}}(E)]^2 \\ & \times \left\{ \sum_{\zeta \geq 1} (\zeta!)^{-2} 2\zeta \binom{N}{2}^{-\zeta} [H e_{\zeta-1}(\hat{E})]^2 \right\} \\ \xrightarrow{\hat{E}=0} & \frac{1}{\pi} \frac{\binom{N+m-1}{m}^2}{\binom{N}{2}} \left\{ 1 + \frac{1}{12} \binom{N}{2}^{-2} + \frac{1}{320} \binom{N}{2}^{-4} + \dots \right\}. \quad (9.30) \end{aligned}$$

Thus, just as for fermions (see Chap. 4), as  $\zeta$  increases, deviations in  $\overline{(\delta E)^2}$  from the leading term rapidly go to zero due to the  $\binom{N}{2}^{-2r}$ ,  $r = 1, 2, \dots$  terms in Eq. (9.30). There will be no change until  $\zeta \sim N/2$ , thereby defining separation. Beyond this, as pointed out first for bosons by Patel et al. [6] using numerical calculations, for  $\zeta \gg N/2$  the deviations grow, i.e. fluctuations set in and they will tend to that of GOE. This is further tested using more numerical calculations in [16]. Comparing Eq. (9.30) with Eq. (4.54), one sees again  $m \leftrightarrow N$  symmetry between dilute fermion and dense boson systems.

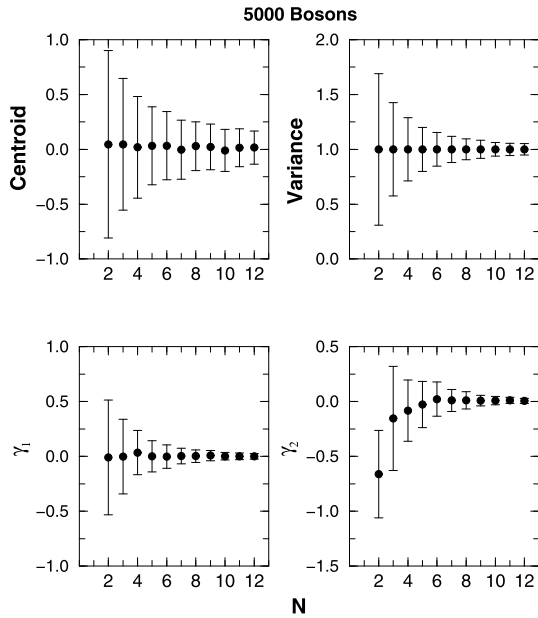
### 9.4.2 Ergodicity in BEGOE(2)

An important question raised by Asaga et al. [8], investigating BEGOE( $k$ ) is that the bosonic ensembles are not ergodic. This was inferred from the study of level fluctuations for large number of bosons in two and three sp states. Turning to boson systems it is seen from Eqs. (9.24) and (9.27), in the dense limit, scaled  $\Sigma_{11}$  and  $\Sigma_{22}$  are

$$\begin{aligned} \hat{\Sigma}_{11} &= \frac{\Sigma_{11}(m)}{\langle H^2 \rangle^m} \rightarrow \frac{4}{N^2}, \\ \hat{\Sigma}_{22} &= \frac{\Sigma_{22}(m)}{\{\langle H^2 \rangle^m\}^2} \rightarrow \frac{16}{N^4} \end{aligned} \quad (9.31)$$

for BEGOE(2) and they remain valid even for BEGOE( $k$ ). Secondly, as  $m \rightarrow \infty$  and  $N$  finite, still the BEGOE( $k$ ) matrix dimension is infinity. Thus, we have a situation where the matrix dimension is infinite and the centroid and variance fluctuations are

**Fig. 9.3** Centroid ( $E_c$ ), variance ( $\sigma^2$ ), skewness ( $\gamma_1$ ) and excess ( $\gamma_2$ ) parameters for the eigenvalue density of a 200 member BEOE(2) systems with 5000 bosons in  $N$  sp states and  $N = 2-12$ . Figure shows average values (filled circle) and widths of the fluctuations (vertical bars) of (a)  $E_c$  normalized by  $\{\sigma^2\}^{1/2}$ , (b)  $\sigma^2$  normalized by  $\sigma^2$ , (c)  $\gamma_1$  and (d)  $\gamma_2$ . Figure is taken from [9] with permission from Elsevier



not zero. Therefore, BEGOE( $k$ ) [similarly BEGUE( $k$ )] is not ergodic if the dense limit is defined by  $m \rightarrow \infty$  and  $N$  finite [1, 8]. However if we follow the definition used in the beginning of this section, then in the dense limit with sufficiently large  $N$  value fluctuations in centroids and variances will tend to zero; see also Fig. 9.3. Going beyond this, fluctuations in  $\gamma_1$  and  $\gamma_2$  have been studied numerically for sufficiently large  $N$  values and very large  $m$  values using the formulas given in Sect. 9.3. As seen from Fig. 9.3, numerical results clearly establish that the variances in  $\gamma_1$  and  $\gamma_2$  rapidly go to zero in the dense limit as  $N$  increases. Thus in the dense limit defined by  $m \rightarrow \infty$ ,  $N \rightarrow \infty$  and  $m/N \rightarrow \infty$ , BEGOE( $k$ ) [also BEGUE( $k$ ) discussed in Chap. 11] will be ergodic [9].

### 9.5 Poisson to GOE Transition in Level Fluctuations: $\lambda_c$ Marker

In Chaps. 5 and 6 it is seen that fermion systems exhibit three transition markers and these play an important role in statistical nuclear spectroscopy and in mesoscopic physics as discussed in Chap. 7. Further applications will be discussed in Chap. 15 ahead. Then, an important questions is: does BEGOE(1 + 2) also exhibit three similar transition markers. This is answered in the affirmative in the present and the next two subsections.

Numerical calculations for  $N = 4, 5$  systems with  $m = 10-12$  have been carried out in [9] and they clearly showed that, as the interaction strength  $\lambda$  in Eq. (9.5) varies, BEGOE(1 + 2) exhibits Poisson to GOE transition in level fluctuations and there is a  $\lambda_c$  marker for this transition just as for EGOE(1 + 2). Figure 9.4 shows

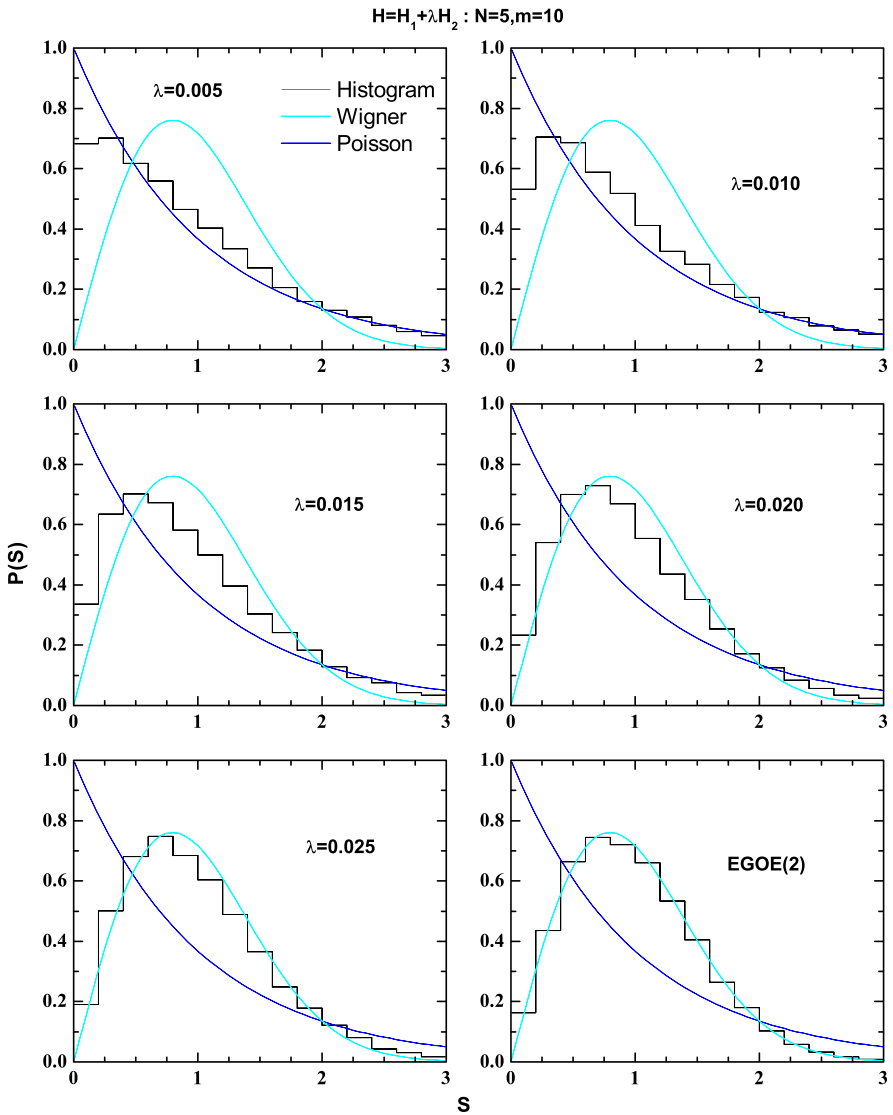
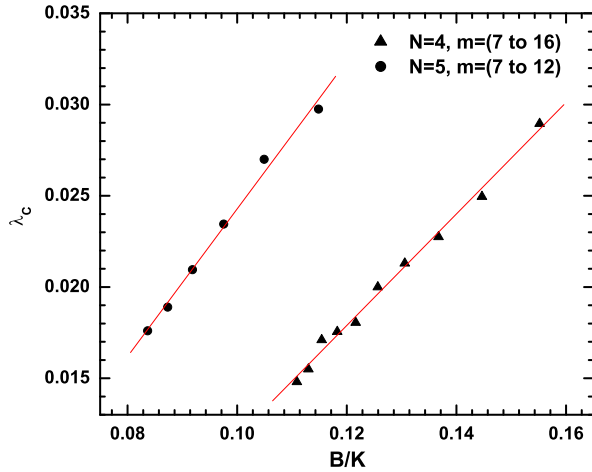


**Fig. 9.4** Ensemble averaged NNSD histogram with  $H = h(1) + \lambda V(2)$ , for various  $\lambda$  values for a BEGOE(1 + 2) system with  $N = 5$  and  $m = 10$ . Note that in the figure,  $H_1 = h(1)$  and  $H_2 = V(2)$ . BEGOE results are compared with Poisson and Wigner (GOE) forms. It is seen clearly that the system exhibits Poisson to GOE transition in NNSD

an example. For  $\lambda = 0$  there are deviations from Poisson form as the sp energies chosen are  $\varepsilon_i = i + 1/i$  (see also Chaps. 5 and 6). The transition marker  $\lambda_c$  can be determined for example by using Eq. (5.18). This gives for example,  $\lambda_c = 0.025$ , 0.018 and 0.015 for  $m = 8$ , 12 and 16 (with  $N = 4$ ) respectively. Similarly,  $\lambda_c =$

**Fig. 9.5** Calculated critical interaction strength  $\lambda_c$  vs  $B/K$ . Filled circles are for  $N = 5$  (with  $m = 7 - 16$ ) and filled triangles are for  $N = 5$  (with  $m = 7 - 12$ ). Figure is taken from [9] with permission from Elsevier (Color figure online)



0.027, 0.021 and 0.018 for  $m = 8, 10$  and  $12$  (with  $N = 5$ ) respectively. In order to verify if  $\lambda_c$  values for BEGOE(1 + 2) follow AJS criterion, an attempt has been made in [9]. According to AJS,  $\lambda_c$  is proportional to the spacing between states directly coupled by  $V(2)$ . With  $B$  giving the span of the directly coupled states ( $B \propto N\Delta$ ) and  $K$  the number of directly coupled states,  $\lambda_c \propto B/K$ . However till now there is no success in deriving a formula for  $K$  for boson systems. In [9],  $K$  is determined by explicit counting in many numerical examples with  $N = 4, 5$ . Plot of  $\lambda_c$  vs  $B/K$ , constructed using this, as shown in Fig. 9.5, verifies that AJS is indeed applicable to BEGOE(1 + 2). It should be noted that though  $\lambda_c$  is proportional to  $B/K$ , the slope is seen to be  $N$  dependent.

## 9.6 BW to Gaussian Transition in Strength Functions: $\lambda_F$ Marker

Strength functions  $F_k(E)$  defined with respect to the basis states  $|k\rangle$ , which are the eigenstates of  $h(1)$  with energy  $E_k = \langle k|H|k\rangle$ , as discussed before in Chap. 5, give information about localization (or delocalization) of the wavefunctions. Just as for fermionic systems (see Chaps. 5 and 6), increasing  $\lambda$  beyond  $\lambda_c$ , it is seen that the strength functions  $F_k(E)$  generated by BEGOE(1 + 2) exhibit BW to Gaussian transition [10] giving a transition marker  $\lambda_F > \lambda_c$ . Figure 9.6 shows an example. In the calculations, strength functions  $F_\xi(E)$  with  $\xi - \delta \leq E_k \leq \xi + \delta$  are averaged and plotted as  $F_\xi(E)$  in Fig. 9.6;  $\delta = 0.025$  for  $\lambda \leq 0.035$  and  $0.1$  for  $\lambda > 0.035$ . The calculated  $F_\xi(E)$  histograms are fitted to a simple function  $F_\xi(E : \mu)$  interpolating

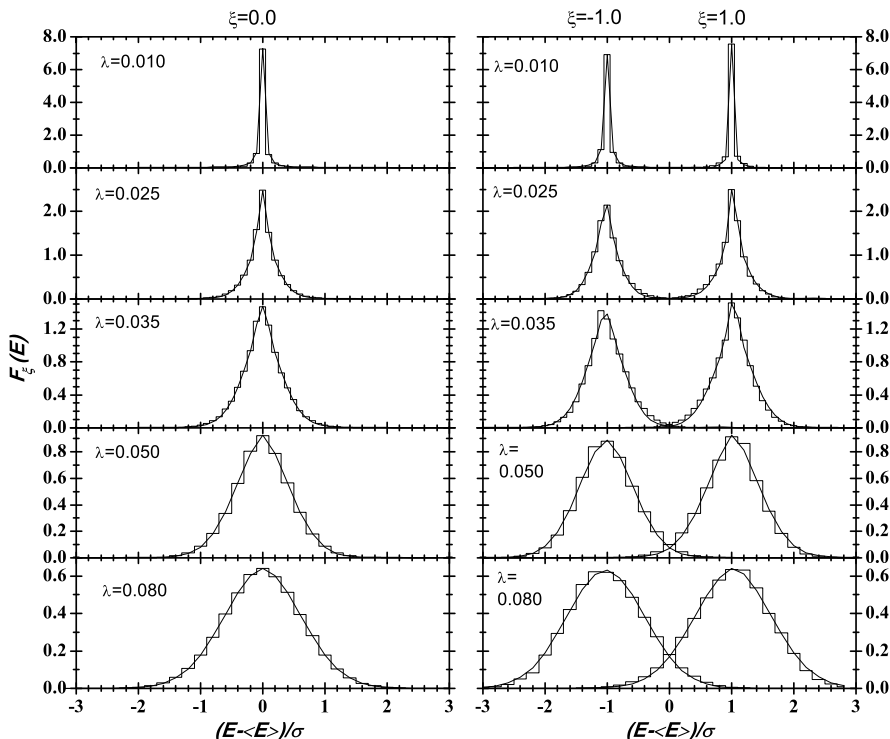


**Fig. 9.6** Ensemble averaged  $F_{\xi}(E)$  histograms for a 20 member BEGOE(1 + 2) with  $N = 5$ ,  $m = 10$ . Results are shown for  $\xi = 0, \pm 1$  and for various  $\lambda$  values. Best fit curves obtained using Eq. (9.32) are also shown for each  $\xi$  and  $\lambda$ . All energies are scaled using  $\sigma$ , the spectral width. It is seen clearly that the system exhibits BW (for very small  $\lambda$ , it is close to a delta-function) to Gaussian transition in strength functions. Figure is taken from [10] with permission from Elsevier

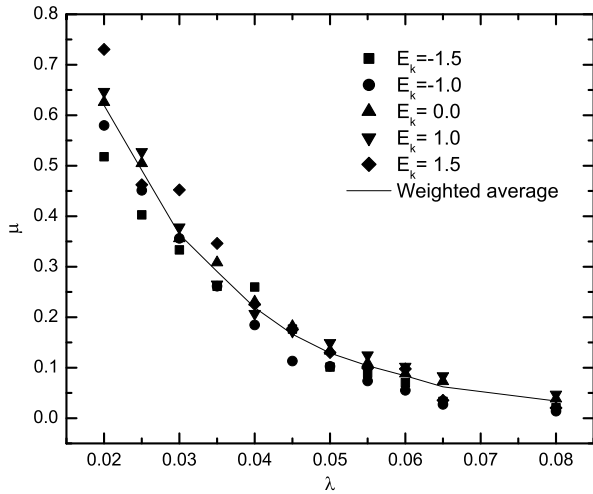
BW and Gaussian forms,

$$\begin{aligned}
 F_{\xi}(E : \mu) &= \mu F_{BW:\xi}(E) + (1 - \mu) F_{\mathcal{G}:\xi}(E); \\
 F_{BW:\xi}(E) &= \frac{1}{2\pi} \frac{\Gamma}{(E - \xi)^2 + \Gamma^2/4}, \\
 F_{\mathcal{G}:\xi}(E) &= \frac{1}{\sqrt{2\pi} \sigma} \exp -(E - \xi)^2/2\sigma^2
 \end{aligned} \tag{9.32}$$

with  $(\mu, \Gamma, \sigma)$  being the free parameters. As seen from Fig. 9.6, the fits are quite good. As  $\mu$  defines the shape of  $F_{\xi}(E)$ , this is the most important parameter in Eq. (9.32). Weighted average of  $\mu$  as a function of  $\lambda$  is shown in Fig. 9.7 and average is calculated as  $\mu = [\sum \mu(\xi) \exp -\xi^2/2]/[\sum \exp -\xi^2/2]$ ;  $\mu(\xi)$  represents  $\mu$ -value that corresponds to  $F_{\xi}(E)$  for a given  $\lambda$ . Using Fig. 9.7 and a criterion for onset of



**Fig. 9.7** Parameter  $\mu$  vs  $\lambda$  for various  $\xi$  values (they are called  $E_k$  in the figure). Continuous curve gives weighted average of  $\mu$ . Figure is taken from [10] with permission from Elsevier



Gaussian behavior, one can deduce the  $\lambda_F$  value. In [10, 20], the criterion used is

$$R(\lambda_F) = 0.7; \quad (9.33)$$

$$R(\lambda) = \frac{\sum_i \{F_\xi^\lambda(E_i) - F_{BW;\xi}(E)\}^2}{\sum_i \{F_{G;\xi}(E_i) - F_{BW;\xi}(E)\}^2}.$$

The interpolating function  $F_\xi(E : \mu)$  gives  $R(\lambda_F) = (1 - \mu^2) = 0.7 \Rightarrow \mu = 0.163$ . Thus, there will be Gaussian behavior for  $\mu \leq 0.163$  with onset at 0.163. This together with the results in Fig. 9.7 give  $\lambda_F \sim 0.05$  for the  $N = 5, m = 10$  system considered in Fig. 9.6. Although we have clear demonstration that as  $\lambda$  going beyond  $\lambda_c$ , strength functions make a transition from BW to Gaussian form in the dense limit of BEGOE(1 + 2), just as with  $\lambda_c$ , there is no formula yet for the  $\lambda_F$  marker in terms of  $(N, m)$ .

## 9.7 Thermalization Region: $\lambda_t$ Marker

### 9.7.1 NPC, $S^{info}$ and $S^{occ}$

As we increase  $\lambda$  beyond  $\lambda_F$ , BEGOE(1 + 2) generates a region of thermalization. Before discussing this, we consider NPC,  $S^{info}$  and  $S^{occ}$  in the dense limit. Firstly, for  $\lambda > \lambda_F$ , it has been well verified that Eq. (5.23) describes NPC in  $h(1)$  basis and similarly Eq. (5.25) for  $\exp(S^{info})$ . Some examples are shown in Figs. 9.8 and 9.9 and given in these figures are also the values of the correlation coefficient  $\zeta$ . In Fig. 9.9,  $S^{info}$  in both  $h(1)$  and  $V(2)$  basis is shown and the importance of this will be discussed ahead. As there is no restriction on number of bosons in a given

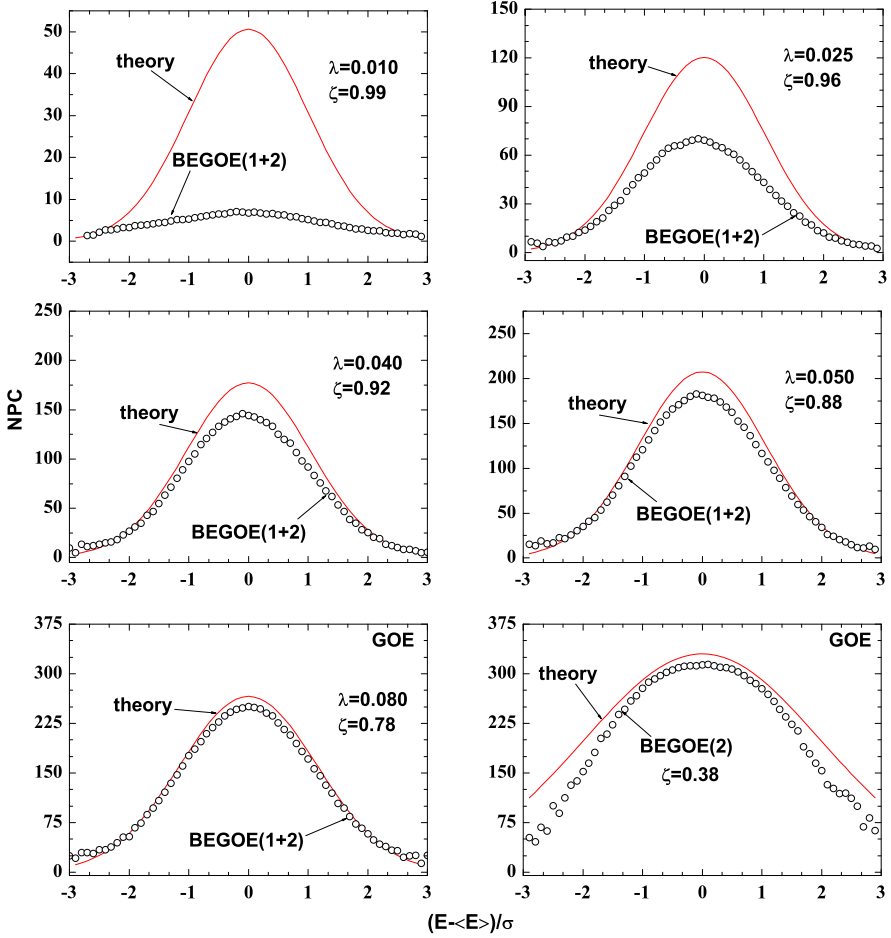


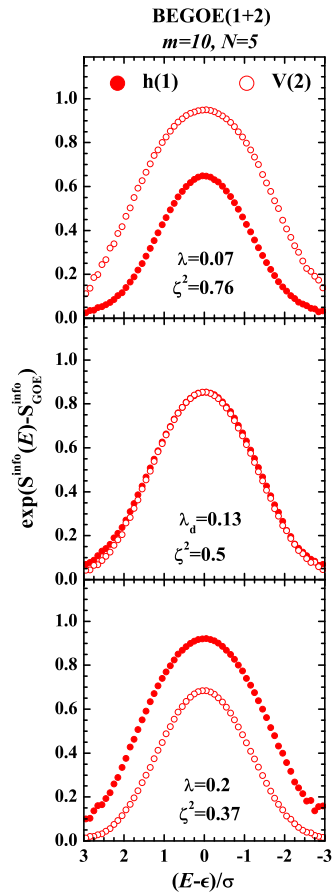
**Fig. 9.8** NPC vs  $E$  for different  $\lambda$  values for a 20 member BEGOE(1 + 2) with  $N = 5, m = 10$ . In the figures ‘theory’ corresponds to Eq. (5.23). Values of  $\zeta$ , the correlation coefficient, are also shown in the figures (Color figure online)

sp level, definition of  $S^{occ}(E)$  will be different for bosons, i.e. Eq. (5.32) will not apply. The definition is,

$$S^{occ}(E) = - \sum_i \langle E | \hat{n}_i | E \rangle \{ \ln \langle E | \hat{n}_i | E \rangle \}. \tag{9.34}$$

Here,  $\langle E | \hat{n}_i | E \rangle$  is the occupancy of the  $i$ -th sp state at energy  $E$ . Applying Eq. (5.31) and carrying out simplifications by treating  $\varepsilon_i$  as a continuous variable, formula for

**Fig. 9.9** Information entropy vs  $E$  in the  $h(1)$  and  $V(2)$  basis for a 100 member BEGOE(1 + 2) ensemble with  $N = 5, m = 10$  for different  $\lambda$  values. Results averaged over bin size 0.1 are shown as *circles*; *filled circles* correspond to  $h(1)$  basis and *open circles* correspond to  $V(2)$  basis. Ensemble averaged  $\zeta^2$  values are also given in the figure. Note that at the duality point  $\lambda = \lambda_d$ , the results in  $h(1)$  and  $V(2)$  basis coincide. Although not shown in the figures, the BEGOE(1 + 2) results follow Eq. (5.25). See Sect. 9.7.2 for details. Figure is constructed using the results in [21] (Color figure online)



$S^{occ}(E)$ , valid in the  $\lambda > \lambda_F$  has been derived in [9] giving

$$\exp\{S^{occ}(E) - \exp S^{occ: max}\} = \exp - \left[ \left( \frac{N+m}{N} \right) \frac{\zeta^2 \hat{E}^2}{2} \right]. \quad (9.35)$$

Result of Eq. (9.35) is compared with numerical examples in Fig. 9.10.

In order to apply the formulas for NPC,  $S^{info}$  and  $S^{occ}$ , we need the correlation coefficient  $\zeta$  and it is defined by Eq. (5.21). Formula for this follows from the results in Sect. 9.2 and the fact that number of off-diagonal and diagonal two-particle matrix elements are  $N(N+1)(N+2)(N-1)/4$  and  $N(N+1)/2$  respectively. Secondly, for the  $V(2)$  matrix, variance of the these off-diagonal elements is  $\lambda^2$  while that of the diagonal elements is  $2\lambda^2$ . Then we have,

$$\zeta^2(m, N) = \frac{\frac{m(N+m)}{N(N+1)} \sum_i \tilde{\epsilon}_i^2 + \lambda^2 \left\{ \frac{m(m-1)(N+m)(N+m+1)}{(N+2)(N+3)} \right\}}{\frac{m(N+m)}{N(N+1)} \sum_i \tilde{\epsilon}_i^2 + \lambda^2 \left\{ \frac{m(m-1)(N+m)(N+m+1)(N^2+N+2)}{4(N+2)(N+3)} \right\}}. \quad (9.36)$$

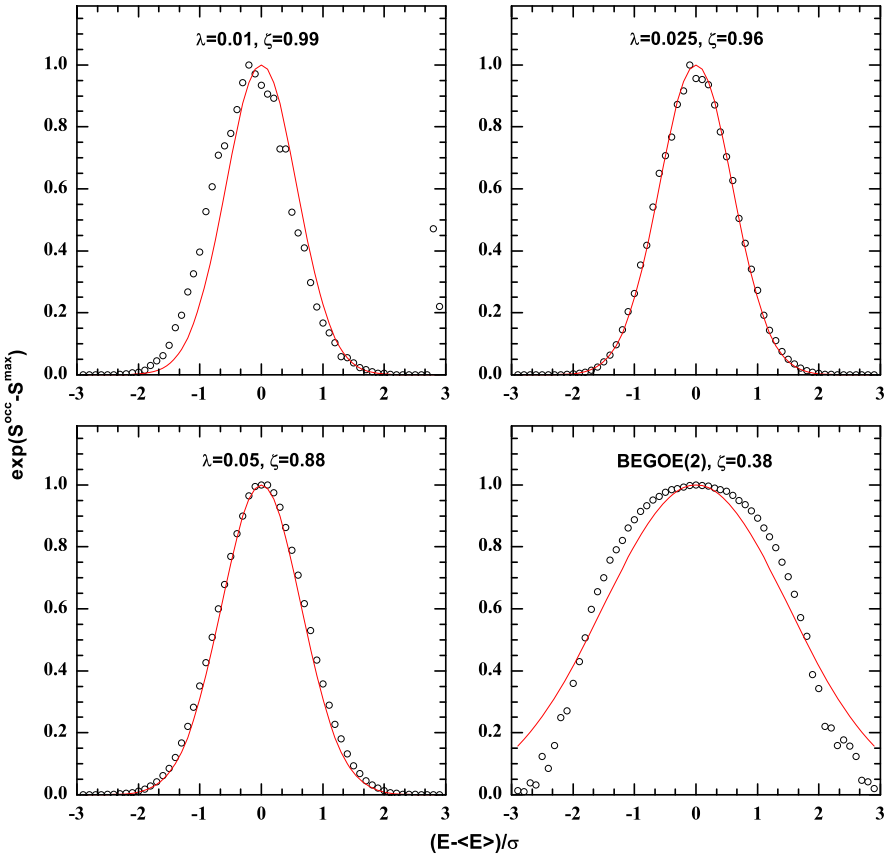


**Fig. 9.10**  $S^{occ}$  vs  $E$  for the same system used in Fig. 9.8. In the figure, *open circles* correspond to the results from the ensemble calculations and the *continuous (red) curves* correspond to Eq. (9.35). Ensemble averaged  $\zeta$  values are also given in the figure (Color figure online)

Numerical calculations in [10] showed that Eq. (9.36) is good for any  $\lambda$ .

### 9.7.2 Thermalization in BEGOE(1 + 2)

Thermalization in interacting boson systems was investigated by Borgonovi et al. [22], using a simple symmetrized coupled two-rotor model. They explored different definitions of temperature and compared the occupancy number distribution with the Bose-Einstein distribution. Their conclusion is: “For chaotic eigenstates, the distribution of occupation numbers can be approximately describe by the Bose-Einstein distribution, although the system is isolated and consists of two particles only. In this case a strong enough interaction plays the role of a heat bath, thus leading to ther-

malization". In order to establish that this is a generic property of interacting boson systems, thermalization in BEGOE(1 + 2) was investigated in [21] using different definitions of temperature and entropy and the results are as follows.

Temperature can be defined in a number of different ways in the standard thermodynamical treatment. These definitions of temperature are known to give same result in the thermodynamical limit i.e. near a region where thermalization occurs [23]. Four definitions of temperature ( $T = \beta^{-1}$ ) are:

- $\beta_c$ : defined using the canonical expression between energy and temperature,

$$\langle E \rangle_{\beta_c} = \frac{\sum_i E_i \exp[-\beta_c E_i]}{\sum_i \exp[-\beta_c E_i]} \quad (9.37)$$

where  $E_i$  are the eigenvalues of the Hamiltonian.

- $\beta_{fit}$ : defined using occupation numbers obtained by making use of the standard canonical distribution,

$$\langle n_k \rangle^E = \frac{\sum_i \langle n_k \rangle^{E_i} \exp[-\beta_{fit} E_i]}{\sum_i \exp[-\beta_{fit} E_i]}. \quad (9.38)$$

Here  $k$  is single particle state index and  $E_i$  are eigenvalues. In applying Eq. (9.38), the constraint  $\sum_k \langle n_k \rangle^E = m$  should be taken into account.

- $\beta_{BE}$ : defined using Bose-Einstein distribution for the occupation numbers,

$$\langle n_k \rangle^E = 1 / \{ \exp[\beta_{BE}(E)(\epsilon_k - \mu(E))] - 1 \}. \quad (9.39)$$

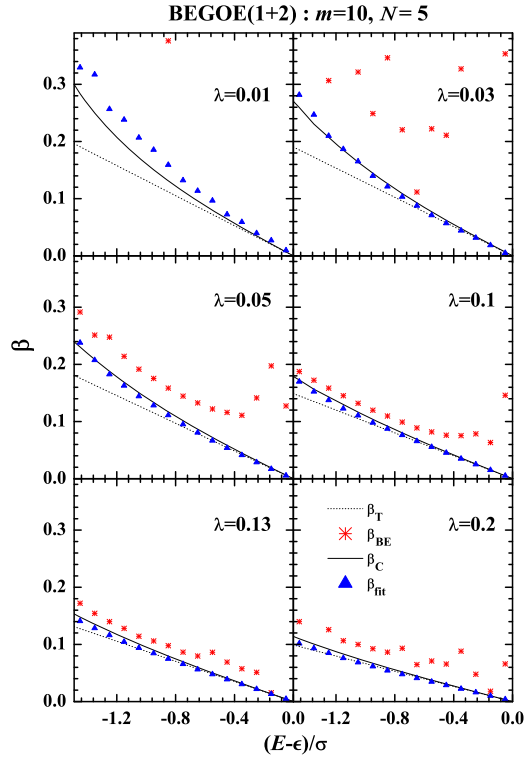
Here  $\mu$  is the chemical potential. Although, this expression is derived for a system with large number of non-interacting particles in contact with a thermostat, it can be used even in isolated systems with relatively few particles [24, 25].

- $\beta_T$ : defined using state density  $\rho(E)$  generated by  $H$ . Note that

$$\beta_T = \frac{d \ln[\rho(E)]}{dE}. \quad (9.40)$$

Figure 9.11 shows ensemble averaged values of  $\beta$ , computed via various definitions described above, for a 100 member BEGOE(1 + 2) ensemble with  $m = 10$  and  $N = 5$  as a function of  $\hat{E} = (E - \epsilon)/\sigma$ , for various  $\lambda$  values. The  $\beta$  values are calculated from  $\hat{E} = -1.5$  to the center of the spectrum, where temperature is infinity. The edges of the spectrum have been avoided as (i) density of states is small near the edges of the spectrum and (ii) eigenstates near the edges are not fully chaotic. Since the state density for BEGOE(1 + 2) is Gaussian irrespective of  $\lambda$  values,  $\beta_T$  as a function of energy gives straight line. Dotted lines shown in the plots represents  $\beta_T$  results in Fig. 9.11. It is clearly seen that for  $\lambda < \lambda_c$  [for  $(m, N) = (10, 5)$ ,  $\lambda_c \sim 0.02$  and  $\lambda_F \sim 0.05$ ], all the definitions give different values of  $\beta$ . Whereas in the region  $\lambda \leq \lambda_F$ , temperature found from BE distribution,  $\beta_{BE}$ , turns out to be completely different from other temperatures. As in this region, the structure of eigenstates is not chaotic enough leading to strong variation in the distribution of the occupation

**Fig. 9.11** Ensemble averaged inverse of temperature  $\beta$  as a function energy  $E$ , for different values of two body interaction strength  $\lambda$  for the BEGOE(1 + 2) system considered in Fig. 9.9. Results for different definitions of inverse of temperature  $\beta$  are given. In the calculations, the sp energies are chosen to be independent Gaussian random variables. With some modification, figure is taken from [21] with permission from Elsevier



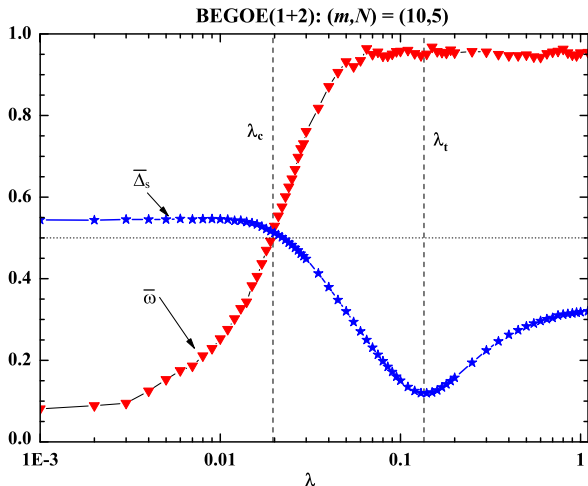
numbers and therefore strong fluctuations in  $\beta_{BE}$ . Moreover, near the center of the spectrum (i.e. as  $T \rightarrow \infty$ ), value of the denominator in Eq. (9.39) becomes very small, which leads to large variation in  $\beta_{BE}$  values from member to member. Further increase in  $\lambda > \lambda_F$ , in the chaotic region, all definitions give essentially same value for the temperature for  $\lambda \sim \lambda_t$ . It is seen from Fig. 9.11 that the matching between different values of  $\beta$  is good near  $\lambda = \lambda_t = 0.13$  for the  $N = 5, m = 10$  example.

For further establishing that  $\lambda \sim \lambda_t$  defines thermodynamic region, used are three different definitions of entropy and these are [as in EGOE(1 + 2) and EGOE(1 + 2)-s studies] thermodynamic entropy  $S^{ther}$ , information entropy  $S^{info}$  and occupancy entropy  $S^{occ}$ . The following measure, introduced in [26] (see also Chap. 15) has been used to obtain  $\lambda_t$ :

$$\Delta_s(\lambda) = \left\{ \int_{-\infty}^{\infty} [(R_E^{info} - R_E^{ther})^2 + (R_E^{sp} - R_E^{ther})^2] dE \right\}^{1/2} / \left\{ \int_{-\infty}^{\infty} R_E^{ther} dE \right\}, \quad (9.41)$$

where  $R_E^\alpha = \exp[S^\alpha(E) - S_{max}^\alpha]$ . In the thermodynamic region the values of the different entropies should be very close to each other, hence the minimum of  $\Delta_s$  gives the value of  $\lambda_t$ . In Fig. 9.12, results shown for ensemble averages  $\overline{\Delta_s}(\lambda)$  (blue stars) obtained for a 100 member BEGOE(1 + 2) ensemble with 10 bosons in 5 single particle states as a function of the two-body interaction strength  $\lambda$ . The second

**Fig. 9.12** Ensemble averaged values  $\overline{\omega}$  and  $\overline{\Delta_s}$  as a function of two body interaction strength  $\lambda$  for the BEGOE(1 + 2) system considered in Fig. 9.9. The vertical dashed lines represent the position of  $\lambda_c$  and  $\lambda_t$ . In the calculation single particle energies are taken as independent real Gaussian random variables. Here  $\lambda_c \simeq 0.02$  and  $\lambda_t \simeq 0.13$ . Figure is taken from [21] with permission from Elsevier (Color figure online)



vertical dashed line indicates the position of  $\lambda_t$  where ensemble averaged  $\overline{\Delta_s(\lambda)}$  is minimum. For the present example, we obtained  $\lambda_t \simeq 0.13$ . This value of  $\lambda_t$  is same as obtained using different definitions of temperature. In order to show that  $\lambda_c \ll \lambda_t$ , the NNSD as a function of  $\lambda$  are fitted to Brody distribution and extracted the Brody parameter  $\omega$ . Then the chaos marker  $\lambda_c$  is determined by the condition  $\omega(\lambda) = 1/2$ . Ensemble averaged values of  $\overline{\omega(\lambda)}$  are shown in Fig. 9.12 and the  $\lambda_c$  value is shown by a vertical dash line in the figure.

To derive a formula for  $\lambda_t$ , considered is duality in BEGOE(1 + 2). The duality region (see Chaps. 5 and 6)  $\lambda = \lambda_d$  is the region (in  $\lambda$  space) where all wave functions look alike and it is expected to correspond to the thermodynamic region defined by  $\lambda = \lambda_t$ . To examine duality,  $S^{info}(E)$  in  $h(1)$  basis and in  $V(2)$  basis are compared. Figure 9.9 shows some numerical results and it is seen that the values of  $S^{info}(E)$  in these two basis coincide at  $\lambda = 0.13$  giving value for the duality marker  $\lambda_d \simeq 0.13$  for the  $N = 5, m = 10$  example. This value is very close to the value of marker  $\lambda_t$  and therefore,  $\lambda_d$  region can be interpreted as the thermodynamic region in the sense that all different definitions of temperature and entropy coincide in this region. As discussed in Sect. 5.3.5,  $\lambda_t$  is given by  $\zeta^2(\lambda_t) = 0.5$ . In addition, Eq. (9.36) gives the  $(m, N)$  dependence of the marker,

$$\lambda_t = 2\sqrt{\frac{(N + 2)X}{N(N + 1)(N - 2)(m - 1)(N + m - 1)}}, \quad X = \sum_{i=1}^N \tilde{\varepsilon}_i^2. \quad (9.42)$$

For uniform sp spectrum with  $\varepsilon_i = i$ ,  $X = N(N + 1)(N - 1)/12$  and then,

$$\lambda_t = \sqrt{\frac{(N - 1)(N + 2)}{3(N - 2)(m - 1)(N + m + 1)}}.$$

For  $m = 10$  and  $N = 5$ , this gives  $\lambda_t \approx 0.15$ . For the sp energies that are used in the calculations in Figs. 9.11 and 9.12,  $X = N(N^2 + 5)/12$  and then

$$\lambda_t = \sqrt{\frac{(N+2)(N^2+5)}{3(N+1)(N-2)(m-1)(N+m+1)}}.$$

For  $m = 10$  and  $N = 5$ , this gives  $\lambda_t \approx 0.16$  as compared to the numerically found value  $\lambda_t = 0.13$ . In the dense limit, Eq. (9.42) gives  $\lambda_t \sim \frac{1}{m} \sqrt{\frac{N}{3}}$ . Similarly, in the dilute limit, it gives  $\lambda_t \sim \frac{1}{\sqrt{3m}}$  in agreement with the EGOE(1 + 2) result given in Chap. 5.

## References

1. T. Asaga, L. Benet, T. Rupp, H.A. Weidenmüller, Spectral properties of the  $k$ -body embedded Gaussian ensembles of random matrices for bosons. *Ann. Phys. (N.Y.)* **298**, 229–247 (2002)
2. F. Iachello, A. Arima, *The Interacting Boson Model* (Cambridge University Press, Cambridge, 1987)
3. F. Iachello, R.D. Levine, *Algebraic Theory of Molecules* (Oxford University Press, New York, 1995)
4. A. Frank, P. Van Isacker, *Algebraic Methods in Molecular and Nuclear Physics* (Wiley, New York, 1994)
5. V.K.B. Kota, Group theoretical and statistical properties of interacting boson models of atomic nuclei: recent developments, in *Focus on Boson Research*, ed. by A.V. Ling (Nova Science Publishers Inc., New York, 2006), pp. 57–105
6. K. Patel, M.S. Desai, V. Potbhare, V.K.B. Kota, Average-fluctuations separation in energy levels in dense interacting boson systems. *Phys. Lett. A* **275**, 329–337 (2000)
7. M. Vyas, Some studies on two-body random matrix ensembles, Ph.D. Thesis, M.S. University of Baroda, India (2012)
8. T. Asaga, L. Benet, T. Rupp, H.A. Weidenmüller, Non-ergodic behaviour of the  $k$ -body embedded Gaussian random ensembles for bosons. *Europhys. Lett.* **56**, 340–346 (2001)
9. N.D. Chavda, V. Potbhare, V.K.B. Kota, Statistical properties of dense interacting Boson systems with one plus two-body random matrix ensembles. *Phys. Lett. A* **311**, 331–339 (2003)
10. N.D. Chavda, V. Potbhare, V.K.B. Kota, Strength functions for interacting bosons in a mean-field with random two-body interactions. *Phys. Lett. A* **326**, 47–54 (2004)
11. M. Vyas, N.D. Chavda, V.K.B. Kota, V. Potbhare, One plus two-body random matrix ensembles for boson systems with  $F$ -spin: analysis using spectral variances. *J. Phys. A, Math. Theor.* **45**, 265203 (2012)
12. V.K.B. Kota, V. Potbhare, Shape of the eigenvalue distribution for bosons in scalar space. *Phys. Rev. C* **21**, 2637–2642 (1980)
13. V.K.B. Kota, A symmetry for the widths of the eigenvalue spectra of boson and fermion systems. *J. Phys. Lett.* **40**, L579–L582 (1979)
14. V.K.B. Kota, Studies on the goodness of IBA group symmetries: centroids, widths and partial widths for irreducible representations of IBA group symmetries. *Ann. Phys. (N.Y.)* **134**, 221–258 (1981)
15. P. Cvitanovic, A.D. Kennedy, Spinors in negative dimensions. *Phys. Scr.* **26**, 5–14 (1982)
16. R.J. Leclair, R.U. Haq, V.K.B. Kota, N.D. Chavda, Power spectrum analysis of the average-fluctuation density separation in interacting particle systems. *Phys. Lett. A* **372**, 4373–4378 (2008)



17. B.J. Dalton, S.M. Grimes, J.P. Vary, S.A. Williams (eds.), *Moment Methods in Many Fermion Systems* (Plenum, New York, 1980)
18. S.S.M. Wong, *Nuclear Statistical Spectroscopy* (Oxford University Press, New York, 1986)
19. N.D. Chavda, Study of random matrix ensembles for bosonic systems, Ph.D. Thesis, M.S. University of Baroda, Vadodara, India (2004)
20. V.K.B. Kota, R. Sahu, Breit-Wigner to Gaussian transition in strength functions, [arXiv:nucl-th/0006079](https://arxiv.org/abs/nucl-th/0006079)
21. N.D. Chavda, V.K.B. Kota, V. Potbhare, Thermalization in one- plus two-body ensembles for dense interacting boson systems. *Phys. Lett. A* **376**, 2972–2976 (2012)
22. F. Borgonovi, I. Guarneri, F.M. Izrailev, G. Casati, Chaos and thermalization in a dynamical model of two interacting particles. *Phys. Lett. A* **247**, 140–144 (1998)
23. M. Rigol, V. Dunjko, M. Olshanii, Thermalization and its mechanism for generic isolated quantum systems. *Nature (London)* **452**, 854–858 (2008)
24. V.V. Flambaum, F.M. Izrailev, Statistical theory of finite Fermi systems based on the structure of chaotic eigenstates. *Phys. Rev. E* **56**, 5144–5159 (1997)
25. V.V. Flambaum, G.F. Gribakin, F.M. Izrailev, Correlations within eigenvectors and transition amplitudes in the two-body random interaction model. *Phys. Rev. E* **53**, 5729–5741 (1996)
26. V.K.B. Kota, A. Relaño, J. Retamosa, M. Vyas, Thermalization in the two-body random ensemble, *J. Stat. Mech.* P10028 (2011)